Nonequilibrium Dynamics of Deconfined Quantum Critical Point in Imaginary Time

Yu-Rong Shu,[1] Shao-Kai Jian,[2] and Shuai Yin[3,*]

[1] *School of Physics and Materials Science, Guangzhou University, Guangzhou 510006, China*
[2] *Condensed Matter Theory Center, Department of Physics, University of Maryland, College Park, Maryland 20742, USA*
[3] *School of Physics, Sun Yat-Sen University, Guangzhou 510275, China*

(Received 24 March 2021; revised 7 October 2021; accepted 24 December 2021; published 12 January 2022)

Deconfined quantum critical point (DQCP) characterizes a kind of exotic phase transition beyond the usual Landau-Ginzburg-Wilson paradigm. Here we study the nonequilibrium imaginary-time dynamics of the DQCP in the two-dimensional J-Q_3 model. We explicitly show the deconfinement dynamic process and identify that it is the spinon confinement length, rather than the usual correlation length, that increases proportionally to the time. Moreover, we find that, in the relaxation process, the order parameters of the Néel and the valence-bond-solid orders can be controlled by different length scales, although they satisfy the same equilibrium scaling forms. A dual dynamic scaling theory is then proposed. Our findings not only constitute a new realm of nonequilibrium criticality in DQCP, but also offer a controllable knob by which to investigate the dynamics in strongly correlated systems. Possible realizations in foreseeable quantum computers are also discussed.

DOI: 10.1103/PhysRevLett.128.020601

Introduction.—Fractionalization is one of the most intriguing notions in particle physics and modern condensed matter physics [1–4]. A prominent example in which fractionalized degrees of freedom play dominant roles is the deconfined quantum critical point (DQCP). The DQCP was proposed to describe the phase transition between the Néel order and the spontaneously dimerized valence-bond solid (VBS) in the two-dimensional (2D) spin-1/2 Heisenberg model [5,6]. According to the traditional Landau-Ginzburg-Wilson (LGW) paradigm, this phase transition should be first ordered. However, the DQCP theory shows that the phase transition can be continuous when the essential fluctuating modes near this critical point are the deconfined spinons and the emergent gauge fields, although the usual "intact" spin-wave and triplet excitations govern the dynamics in the Néel and VBS order, respectively [5,6]. Besides its conceptual importance, the DQCP also provides profound insights in other strongly correlated systems, such as high-temperature superconductivity [7–10], spin liquid [11–13], lattice gauge theory [14–17], and so on. Accordingly, the DQCP has attracted enormous attention from theoretical, numerical, and experimental aspects [18–39].

The long-range fluctuations of the deconfined degrees of freedom can induce striking equilibrium critical properties near the DQCP. Besides the remarkably large anomalous dimension [20,25], the DQCP possesses two relevant length scales. In addition to the correlation length scale ξ, an extra divergent length ξ', which measures the spinon confinement length or the thickness of the VBS domain walls, develops near the DQCP [6,30]. They satisfy $\xi' \propto \xi^{(\nu'/\nu)}$, with ν and ν' being the corresponding critical exponents [6,30]. It was plausibly shown that the interplay between these two length scales may take responsibility for some anomalous equilibrium scaling behaviors near the DQCP [29,30].

On the other hand, understanding nonequilibrium dynamics is one of the central subjects in diverse fields such as cosmology, high-energy physics, and condensed matter physics, spanning almost all time and length scales [40,41]. Near a critical point, the nonequilibrium dynamics has been raising intensive attention from both theoretical [40,41] and experimental aspects [42–45]. However, the nonequilibrium critical dynamics in the 2D DQCP has rarely been studied.

As a routine method to find the ground state, the imaginary-time evolution is now under extensive investigation owing to its application in the experimental platforms of quantum computers [46–49], which were shown to provide a promising tool to study the nonequilibrium properties ranging from high-energy physics to quantum critical dynamics [50–55]. In addition, the imaginary-time dynamics shares some universal properties with the real-time dynamics and bears amenability to quantum Monte Carlo (QMC) simulations without sign problem [56–58]. Previous studies demonstrated that the imaginary-time relaxation dynamics in the LGW quantum phase transitions [59] exhibits scaling behaviors in analogy to the classical short-time critical dynamics [60–62], providing fruitful insights in quantum critical dynamics [59,63–66].

These motivate us to study the imaginary-time relaxation dynamics of the DQCP. By large-scale QMC simulations [58,67,68], we show that the DQCP exhibits a lot of exotic nonequilibrium scaling behaviors induced by the intriguing interplay between the nonequilibrium dynamics, deconfinement process, emergent symmetry, and the critical scaling with the two length scales. In particular, we find that it is the spinon confinement length ξ', rather than the conventional correlation length ξ, that scales with the imaginary time τ as $\xi' \propto \tau^{(1/z)}$ with $z = 1$ as the dynamic exponent in DQCP, in sharp contrast to the usual LGW critical dynamics in which $\xi \propto \tau^{(1/z)}$ [59,63]. In addition, we find the dynamics of the Néel order parameter and the VBS order parameter can be controlled by different length scales, although they share similar equilibrium finite-size scaling. Moreover, a remarkable dual dynamic scaling is then discovered, in which the scaling form of the Néel order parameter and the VBS order parameter exchanges as the initial state is changed to its dual counterpart. This dual dynamic scaling can be regarded as the nonequilibrium incarnation of the equilibrium emergent symmetry.

Model.—A prototypical model that exhibits the DQCP is the J-Q_3 model in the 2D square lattice [20]. The Hamiltonian reads

$$H = -J\sum_{\langle ij\rangle} P_{ij} - Q \sum_{\langle ijklmn\rangle} P_{ij}P_{kl}P_{mn}, \qquad (1)$$

in which $J > 0$ and $Q > 0$, $\langle ij\rangle$ and $\langle ijklmn\rangle$ denote, respectively, nearest neighbors and three nearest-neighbor pairs in horizontal or vertical columns on the square lattice, and P_{ij} denotes the spin singlet operator defined as $P_{ij} \equiv \frac{1}{4} - \mathbf{S}_i \cdot \mathbf{S}_j$ with $\mathbf{S}$ being the spin-1/2 operator. The system favors the Néel (VBS) phase with a finite order parameter M (D) when $q \equiv J/Q \gg 1$ ($\ll 1$) [20]. For the imaginary-time relaxation dynamics, the evolution of the wave function $|\psi(\tau)\rangle$ obeys the imaginary-time Schrödinger equation $-(\partial/\partial\tau)|\psi(\tau)\rangle = H|\psi(\tau)\rangle$ with an uncorrelated initial state [59].

Relaxation dynamics of two length scales.—Given the two relevant length scales in DQCP, one should at first explore their dynamic scalings. Scaling analyses demonstrate that there should be two possibilities: (i) $\xi \propto \tau^{(1/z)}$ and $\xi' \propto \tau^{(\nu'/\nu z)}$; (ii) $\xi' \propto \tau^{(1/z)}$, and $\xi \propto \tau^{(\nu/z\nu')}$. In usual LGW criticality, conventional wisdom tells us that $\xi \propto \tau^{(1/z)}$ [59,63,64], indicating that scenario (i) is right. However, a prominent question is whether this scenario is also selected by the DQCP.

To reveal the answer, we investigate the deconfinement process from an initial state with a triplet embedded in the VBS background at the critical point (determined in the following). We find that the size of the spinon pair Λ, defined via the strings connecting the unpaired spins in the $S = 1$ sector [30,69], increases with τ as $\Lambda \propto \tau^{0.931}$ as shown in Figs. 1(a) and 1(b). This exponent is close to 1, demonstrating that $\xi' \propto \tau^{(1/z)}$, since it was shown that $\xi' \propto \Lambda$ [30]. There follows $\xi \propto \tau^{(1/z_u)}$ with $z_u \equiv (z\nu'/\nu)$ (subscript u indicates the usual length scale). This demonstrates that scenario (ii) is right.

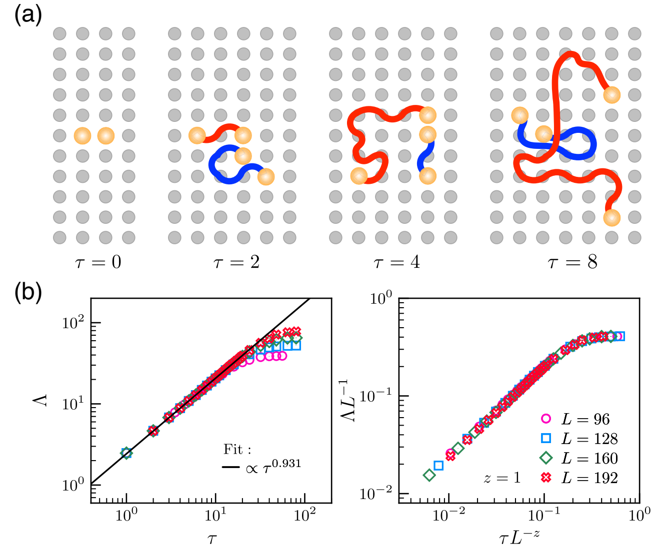

FIG. 1. Dynamics of the confinement length scale. (a) Illustration of the fractionalization process of spinons. Shown is the evolution of typical configurations for a sampled overlap $\langle\psi_{\text{left}}|\psi_{\text{right}}\rangle$ in $S = 1$ sector with two spinon strings, which are initially located in nearest-neighbor sites embedded in the VBS background (not shown). (b) Curves of the size of spinon pair Λ for various lattice sizes before (left) and after (right) rescaling.

General dynamic scaling form.—Generally, the imaginary-time relaxation process near the DQCP should be controlled by the dynamics of two relevant length scales $\xi' \propto \tau^{(1/z)}$ and $\xi \propto \tau^{(1/z_u)}$. For an operator Y, its dynamic scaling should satisfy

$$Y(\tau, \delta, L, \{X\}) = \tau^{\frac{s}{\tilde{z}}} f(\delta\tau^{\frac{1}{\tilde{\nu}\tilde{z}}}, \tau L^{-z}, \tau L^{-z_u}, \{X\tau^{-\frac{c}{\tilde{z}}}\}), \quad (2)$$

in which s is the exponent related to Y, $\delta \equiv q - q_c$ with q_c as the critical point, L is the lattice size, and $\tilde{z}$ is the dynamic exponent, which can be z or z_u, or their combination, depending on the dynamic process; similarly, $\tilde{\nu}$ can be ν or ν', and $\{X\}$ with its exponent c represents other possible relevant variables associated with the initial state [70]. For saturated ordered and completely disordered initial states, X vanishes, since these states keep invariant under scale transformation [59,60]. If $z_u = z$, Eq. (2) recovers the usual single-length-scale relaxation scaling theory, in which, for instance, a dimensionless variable at $\delta = 0$ is a function of τL^{-z_u}, and the order parameter scales as $M^2 = \tau^{-(2\beta/\nu z_u)} f(\tau L^{-z_u})$ for a saturated initial state, and $M^2 = L^{-d}\tau^{(d/z_u)-(2\beta/\nu z_u)} f(\tau L^{-z_u})$ for a disordered initial state [62]. These results are benchmarked in the quantum Ising model [71,72] in the Supplemental Material [73].

Relaxation dynamics with the VBS initial state.—We then explore the dynamic scaling in model (1) from a saturated VBS state. For a dimensionless quantity

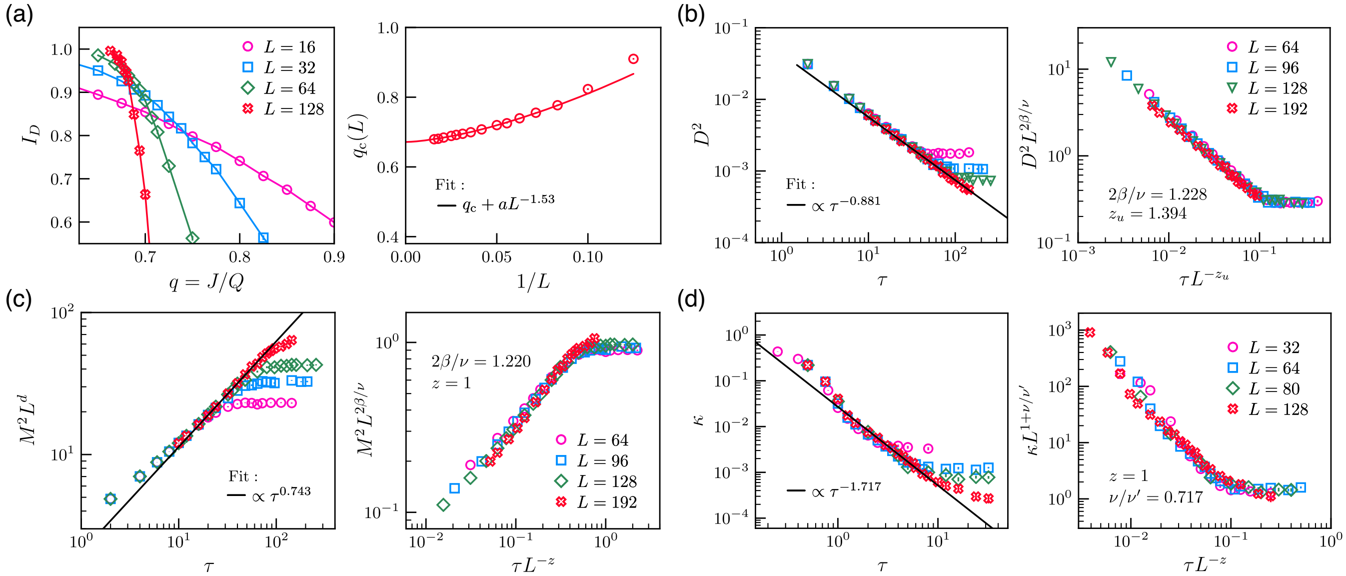

FIG. 2. Relaxation dynamics with the VBS initial state. (a) Determination of the critical point via the average sign of the VBS order parameter I_D. (b) Curves of the squared VBS order parameter for various lattice sizes before (left) and after (right) rescaling. (c) Curves of the squared Néel order parameter for various lattice sizes before (left) and after (right) rescaling. (d) Curves of the density of domain wall energy κ for various lattice sizes before (left) and after (right) rescaling.

$I_D(\tau, \delta, L)$, defined as the average sign of the VBS order parameter, $I_D \equiv \langle \mathrm{sgn}\{D(\tau)\} \rangle$, we find in Fig. 2(a) that for a fixed τL^{-z} the convergence of crossing points of $I_D(\tau, \delta, L)$ for large L corroborates the value of the critical point $q_c \simeq 0.671(2)$ [24], which indicates that τL^{-z} dominates the dynamics of I_D, rather than τL^{-z_u}. This makes the scaling form of I_D remarkably different from the usual one, since the relevant length scale is not the conventional ξ but the spinon confinement length ξ'.

In equilibrium, both M^2 and D^2 are proportional to $L^{-(2\beta/\nu)}$ with $(2\beta/\nu) \simeq 1.228$ [24,27,37]. Strikingly, here we find that their relaxation dynamics from a saturated VBS initial state are controlled by different length scales. For D^2, Fig. 2(b) shows that in the short-time stage it obeys $D^2(\tau, L) = \tau^{-0.881}$, suggesting the exponent is $(2\beta/\nu z_u)$ with $z_u \simeq 1.394$. Accordingly, $\nu/\nu' \simeq 0.717$, close to the known results [30,74]. The short- and long-time scaling behaviors require that the scaling form of D^2 satisfies $D^2(\tau, L) = \tau^{-(2\beta/\nu z_u)} f(\tau L^{-z_u})$, for which the usual correlation length $\xi \propto \tau^{(1/z_u)}$ dominates. Otherwise, if ξ' dominates, the appearance of τL^{-z} in the scaling function f will make the scaling form hard to satisfy these two limits simultaneously within a simple form. The above scaling form is confirmed by the rescaling collapse in Fig. 2(b) [75].

Contrarily, for M^2, Fig. 2(c) shows that its short-time dynamics obeys $M^2 \propto L^{-d}\tau^{0.743}$ [73]. This exponent is close to $[(d/z) - (2\beta/\nu z)]$. Accordingly, the short- and long-time scaling behaviors require the full scaling form of M^2 to be $M^2(\tau, L) = L^{-d}\tau^{(d/z)-(2\beta/\nu z)} f(\tau L^{-z})$, where ξ' and τL^{-z} dominate. This scaling form is confirmed by the scaling collapse in Fig. 2(c). Thus, D^2 and M^2 select different dominant length scales separately. A possible reason for the discrepancy is that D^2 is deeply affected by the memory from the initial VBS state and thus the local fluctuations dominate in the short-time stage; whereas with this initial state M^2 feels a disorder environment and its value comes from the global fluctuations, for which the contributions of VBS domain walls govern the dynamic scaling behaviors [73].

More interestingly, some quantities can even show fascinating relaxation behaviors controlled by the dynamics of ξ and ξ' simultaneously. For instance, in equilibrium, the VBS domain wall energy density κ is found to scale as $\kappa \propto \xi'^{-1}\xi^{-(d+z-2)}$ $(d + z - 2 = 1)$ [5,30]. Here we generalized this scaling into the nonequilibrium case. As shown in Fig. 2(d), κ relaxes according to $\kappa(\tau, L) = \tau^{-(1/z)}\tau^{-(1/z_u)} f(\tau L^{-z})$ from the saturated VBS state at $q = q_c$. In the short-time stage, $\kappa \propto \tau^{-(1/z)}\tau^{-(1/z_u)}$, while in the long-time stage, κ crosses over to $\kappa \sim L^{-[1+(\nu/\nu')]}$ as $f(\tau L^{-z}) \sim (\tau L^{-z})^{(1/z_u)+(1/z)}$ for $\tau \to \infty$, recovering its equilibrium finite-size scaling [6,30,73,74].

Relaxation dynamics with the Néel initial state.—To illustrate the role played by the initial state in the relaxation dynamics, we now study the dynamic scaling with the saturated antiferromagnetic initial state. From Fig. 3(a), we find that the average sign of the Néel order parameter defined as $I_M \equiv \langle \mathrm{sgn}\{M(\tau)\} \rangle$ obeys $I_M = f(\tau L^{-z})$ similar to I_D. The critical point estimated by crossing-point analyses of I_M is 0.671(2), consistent with that given by I_D. Notably, we find that M^2 and D^2 exchange their scaling forms compared with the VBS initial state case.

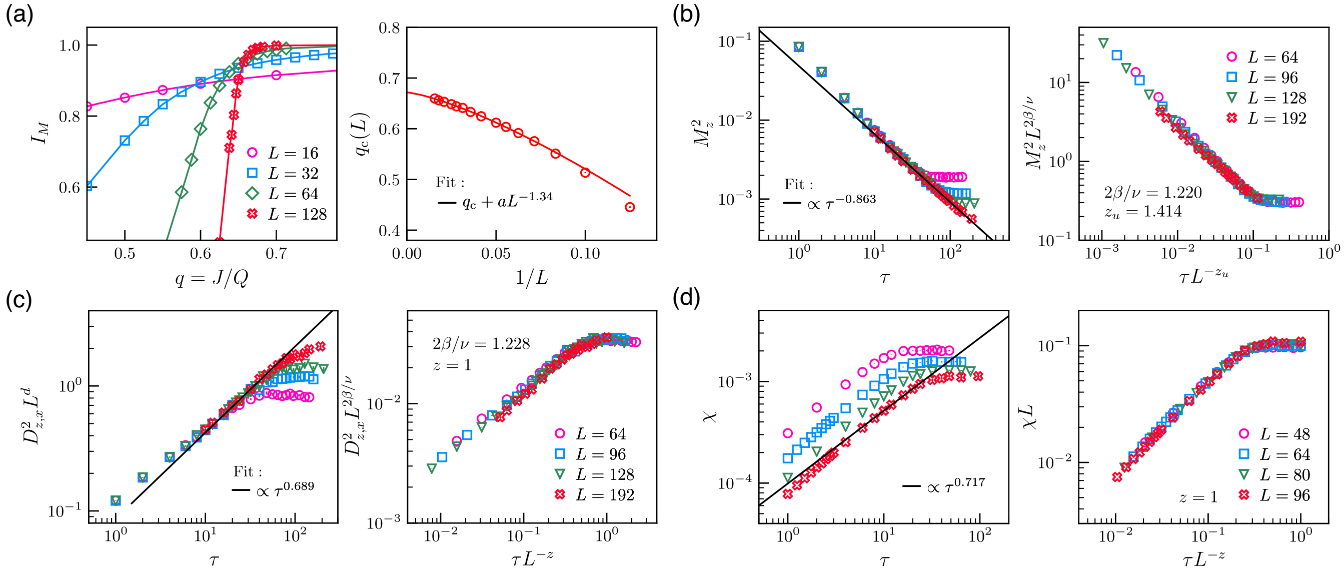

FIG. 3. Relaxation dynamics with the saturated Néel initial state. (a) The average sign of the Néel order parameter I_M is used to estimate the critical point. For different L and fixed $\tau L^{-1} = 1/4$, crossing points (left) of curves of $I_M - q$ are extrapolated to estimate the critical point as $q_c \simeq 0.671(2)$ (right), corroborating that from I_D shown in Fig. 2. (b) Curves of the squared VBS order parameter for various lattice sizes before (left) and after (right) rescaling. (c) Curves of the squared Néel order parameter for various lattice sizes before (left) and after (right) rescaling. (d) Curves of the susceptibility for various lattice sizes before (left) and after (right) rescaling.

Namely, M^2 satisfies $M^2(\tau, L) = \tau^{-(2\beta/\nu z_u)} f(\tau L^{-z_u})$ governed by ξ, since in the short-time stage its dominant component M_z decays as $M_z^2 \propto \tau^{-0.863}$ with the exponent close to $(2\beta/\nu z_u)$, as shown in Fig. 3(b). Contrarily, D^2 satisfies $D^2(\tau, L) = L^{-d} \tau^{(d/z)-(2\beta/\nu z)} f(\tau L^{-z})$, governed by ξ', since D^2 changes as $D^2 \propto L^{-d} \tau^{0.689}$ with the exponent close to $(d/z) - (2\beta/\nu z)$, as shown in Fig. 3(c). Moreover, the full scaling forms for M^2 and D^2 are also verified in Figs. 3(b) and 3(c) by rescaling collapse. Again, M^2 and D^2 are governed by different length scales.

In addition, we find in Fig. 3(d) that the dynamics of the susceptibility χ at the momentum $[(2\pi/L), 0]$ [30] satisfies $\chi(\tau, L) = L^{-(d-z)} f(\tau L^{-z})$ (here $d - z = 1$). An interesting phenomenon is that in the short-time stage $\chi(\tau, L) \sim L^{-1} (\tau L^{-z})^{(\nu/\nu' z)}$, indicating a hidden interplay between the dynamics of two length scales (see Supplemental Material for further discussions [73]).

Dual dynamic scaling.—The exchange of scaling forms for M^2 and D^2 demonstrates a remarkable dual dynamic scaling behavior. This dual dynamic scaling property can be regarded as the dynamic incarnation of the equilibrium emergent symmetry, which, for model (1), is an emergent SO(5) symmetry by the rotation between the Néel order and the VBS order [19,37]. The emergence of the dual dynamic scaling is quite intriguing. As demonstrated in the usual two-length scale theory, the dangerously irrelevant variable and the corresponding additional length scale only manifest themselves in one side of the transition point [76–79]. In the DQCP of model (1), it was regarded that the discrete Z_4 symmetry breaking in the VBS phase takes responsibility for the additional length scale [30,37]. Therefore, asymmetric dynamic behaviors can be expected for different initial conditions. However, here we find that $M^2(D^2)$ for the saturated antiferromagnet initial state shares the same scaling form with $D^2(M^2)$ for the saturated VBS initial state. This demonstrates that the scaling with two length scales even extends to low excited states in both sides of the DQCP.

The dual dynamic scaling also manifests itself when the initial state is a disordered state. We find in the Supplemental Material [73] that M^2 and D^2 evolve according to the same scaling form $P^2(\tau, L) = L^{-d} \tau^{(d/z)-(2\beta/\nu z)} f(\tau L^{-z})$ in which P represents M or D and ξ' dominates their relaxation dynamics.

Discussion.—Our findings can be detected in the experimental platforms of quantum computers in the foreseeable future. Recently, realizing various "experiments" in quantum computers has become a new vivifying realm ranging from high-energy physics [50] to condensed matter physics [51–55], boosted by the claimed quantum advantage [80–82]. In particular, nonequilibrium quantum critical dynamics has been observed in the noisy intermediate-scale quantum device [52]. Moreover, imaginary-time relaxation has been employed in various quantum computational devices in the search of ground states [46–48]. It is promising that the imaginary-time relaxation dynamics we revealed can be detected directly in these devices. Besides, since directly simulating the real-time dynamics in 2D is confronting huge challenges, our work also provides significant instructions to the real-time relaxation dynamics of the DQCP by realizing that the short-time scaling also manifests itself in real-time dynamics in various quantum systems [83–88].

Summary.—In summary, we have studied the imaginary-time nonequilibrium dynamics in 2D DQCP and found that the interplay between the deconfinement process and the fluctuating modes with two length scales can contribute striking nonequilibrium properties. We have identified that in the relaxation process the confinement length ξ' increases proportionally to τ, contrary to the usual case in which ξ increases proportionally to τ. In addition, we have discovered that the Néel and VBS order parameters can be controlled by different length scales, depending on the initial states, although these two order parameters obey the similar equilibrium finite-size scaling. An exotic dual dynamic scaling is then discovered, which can be regarded as the dynamic incarnation of the equilibrium emergent symmetry. In this dual dynamic scaling, the scaling form of the Néel order parameter and the VBS order parameter exchanges as the initial state is changed to its dual counterpart. Our work pioneers the studies on the non-equilibrium dynamics in 2D DQCP and provides new ingredients in investigations on the DQCP. Possible realizations in near-term quantum computers have also been discussed.

We gratefully acknowledge helpful discussions with A. W. Sandvik, H. Shao, P. Ye, F. Zhong, W. Guo, and Z. Y. Meng. Y. R. S. acknowledges support from the National Natural Science Foundation of China (Grants No. 11947035 and No. 12104109), the Science and Technology Projects in Guangzhou (202102020933). S. K. J. is supported by the Simons Foundation via the It From Qubit Collaboration. S. Y. is supported by the National Natural Science Foundation of China (Grant No. 12075324). The numerical analysis was in part performed on TianHe-2 (the National Supercomputer Center in Guangzhou).

*yinsh6@mail.sysu.edu.cn

[1] S. Sachdev, *Quantum Phase Transitions*, 2nd ed. (Cambridge University Press, Cambridge, England, 2011).
[2] X.-G. Wen, *Quantum Field Theory of Many-Body Systems* (Oxford University Press, New York, 2004).
[3] E. Fradkin, *Field Theories of Condensed Matter Physics*, 2nd ed. (Cambridge University Press, Cambridge, England, 2013).
[4] S. Sachdev, Quantum magnetism and criticality, Nat. Phys. **4**, 173 (2008).
[5] T. Senthil, A. Vishwanath, L. Balents, S. Sachdev, and M. P. A. Fisher, Deconfined quantum critical points, Science **303**, 1490 (2004).
[6] T. Senthil, L. Balents, S. Sachdev, A. Vishwanath, and M. P. A. Fisher, Quantum criticality beyond the Landau-Ginzburg-Wilson paradigm, Phys. Rev. B **70**, 144407 (2004).
[7] R. K. Kaul, A. Kolezhuk, M. Levin, S. Sachdev, and T. Senthil, Hole dynamics in an antiferromagnet across a deconfined quantum critical point, Phys. Rev. B **75**, 235122 (2007).
[8] R. K. Kaul, M. A. Metlitski, S. Sachdev, and C. Xu, Destruction of Néel order in the cuprates by electron doping, Phys. Rev. B **78**, 045110 (2008).
[9] R. K. Kaul and S. Sachdev, Quantum criticality of U(1) gauge theories with fermionic and bosonic matter in two spatial dimensions, Phys. Rev. B **77**, 155105 (2008).
[10] Y.-H. Zhang and S. Sachdev, Deconfined criticality and ghost Fermi surfaces at the onset of antiferromagnetism in a metal, Phys. Rev. B **102**, 155124 (2020).
[11] Y. Zhou, K. Kanoda, and T.-K. Ng, Quantum spin liquid states, Rev. Mod. Phys. **89**, 025003 (2017).
[12] L. Savary and L. Balents, Quantum spin liquids: A review, Rep. Prog. Phys. **80**, 016502 (2017).
[13] C. Broholm, R. J. Cava, S. A. Kivelson, D. G. Nocera, M. R. Norman, and T. Senthil, Quantum spin liquids, Science **367**, eaay0668 (2020).
[14] L. Janssen and Y.-C. He, Critical behavior of the QED_3-Gross-Neveu model: Duality and deconfined criticality, Phys. Rev. B **96**, 205113 (2017).
[15] X. Y. Xu, Y. Qi, L. Zhang, F. F. Assaad, C. Xu, and Z. Y. Meng, Monte Carlo Study of Lattice Compact Quantum Electrodynamics with Fermionic Matter: The Parent State of Quantum Phases, Phys. Rev. X **9**, 021022 (2019).
[16] Y. Q. Qin, Y.-Y. He, Y.-Z. You, Z.-Y. Lu, A. Sen, A. W. Sandvik, C. Xu, and Z. Y. Meng, Duality between the Deconfined Quantum-Critical Point and the Bosonic Topological Transition, Phys. Rev. X **7**, 031052 (2017).
[17] L. Janssen, W. Wang, M. M. Scherer, Z. Y. Meng, and X. Y. Xu, Confinement transition in the QED_3-Gross-Neveu-XY universality class, Phys. Rev. B **101**, 235118 (2020).
[18] M. Levin and T. Senthil, Deconfined quantum criticality and Néel order via dimer disorder, Phys. Rev. B **70**, 220403(R) (2004).
[19] T. Senthil and M. P. A. Fisher, Competing orders, nonlinear sigma models, and topological terms in quantum magnets, Phys. Rev. B **74**, 064405 (2006).
[20] A. W. Sandvik, Evidence for Deconfined Quantum Criticality in a Two-Dimensional Heisenberg Model with Four-Spin Interactions, Phys. Rev. Lett. **98**, 227202 (2007).
[21] R. G. Melko and R. K. Kaul, Scaling in the Fan of an Unconventional Quantum Critical Point, Phys. Rev. Lett. **100**, 017203 (2008).
[22] F.-J. Jiang, M. Nyfeler, S. Chandrasekharan, and U.-J. Wiese, From an antiferromagnet to a valence bond solid: Evidence for a first-order phase transition, J. Stat. Mech. (2008) P02009.
[23] A. B. Kuklov, M. Matsumoto, N. V. Prokof'ev, B. V. Svistunov, and M. Troyer, Deconfined Criticality: Generic First-Order Transition in the SU(2) Symmetry Case, Phys. Rev. Lett. **101**, 050405 (2008).
[24] J. Lou, A. W. Sandvik, and N. Kawashima, Antiferromagnetic to valence-bond-solid transitions in two-dimensional SU(N) Heisenberg models with multispin interactions, Phys. Rev. B **80**, 180414(R) (2009).
[25] A. W. Sandvik, Continuous Quantum Phase Transition between an Antiferromagnet and a Valence-Bond Solid in

Two Dimensions: Evidence for Logarithmic Corrections to Scaling, Phys. Rev. Lett. **104**, 177201 (2010).
[26] K. Chen, Y. Huang, Y. Deng, A. B. Kuklov, N. V. Prokof'ev, and B. V. Svistunov, Deconfined Criticality Flow in the Heisenberg Model with Ring-Exchange Interactions, Phys. Rev. Lett. **110**, 185701 (2013).
[27] K. Harada, T. Suzuki, T. Okubo, H. Matsuo, J. Lou, H. Watanabe, S. Todo, and N. Kawashima, Possibility of deconfined criticality in SU(N) Heisenberg models at small N, Phys. Rev. B **88**, 220408(R) (2013).
[28] S. Pujari, K. Damle, and F. Alet, Néel-State to Valence-Bond-Solid Transition on the Honeycomb Lattice: Evidence for Deconfined Criticality, Phys. Rev. Lett. **111**, 087203 (2013).
[29] A. Nahum, J. T. Chalker, P. Serna, M. Ortuño, and A. M. Somoza, Deconfined Quantum Criticality, Scaling Violations, and Classical Loop Models, Phys. Rev. X **5**, 041048 (2015).
[30] H. Shao, W. Guo, and A. W. Sandvik, Quantum criticality with two length scales, Science **352**, 213 (2016).
[31] M. E. Zayed *et al.*, 4-spin plaquette singlet state in the Shastry-Sutherland compound $SrCu_2(BO_3)_2$, Nat. Phys. **13**, 962 (2017).
[32] C. Wang, A. Nahum, M. A. Metlitski, C. Xu, and T. Senthil, Deconfined Quantum Critical Points: Symmetries and Dualities, Phys. Rev. X **7**, 031051 (2017).
[33] B. Ihrig, N. Zerf, P. Marquard, I. F. Herbut, and M. M. Scherer, Abelian Higgs model at four loops, fixed-point collision, and deconfined criticality, Phys. Rev. B **100**, 134507 (2019).
[34] N. Ma, Y.-Z. You, and Z. Y. Meng, Role of Noether's Theorem at the Deconfined Quantum Critical Point, Phys. Rev. Lett. **122**, 175701 (2019).
[35] Y. Liu, Z. Wang, T. Sato, M. Hohenadler, C. Wang, W. Guo, and F. F. Assaad, Superconductivity from the condensation of topological defects in a quantum spin-Hall insulator, Nat. Commun. **10**, 2658 (2019).
[36] Z.-X. Li, S.-K. Jian, and H. Yao, Deconfined quantum criticality and emergent SO(5) symmetry in fermionic systems, arXiv:1904.10975.
[37] A. Nahum, P. Serna, J. T. Chalker, M. Ortuño, and A. M. Somoza, Emergent SO(5) Symmetry at the Néel to Valence-Bond-Solid Transition, Phys. Rev. Lett. **115**, 267203 (2015).
[38] Y.-C. Wang, N. Ma, M. Cheng, and Z. Y. Meng, Scaling of disorder operator at deconfined quantum criticality, arXiv:2106.01380.
[39] J. Zhao, Y.-C. Wang, M. Cheng, and Z. Y. Meng, Scaling of Entanglement Entropy at Deconfined Quantum Criticality, Phys. Rev. Lett. **128**, 010601 (2022).
[40] J. Dziarmaga, Dynamics of a quantum phase transition and relaxation to a steady state, Adv. Phys. **59**, 1063 (2010).
[41] A. Polkovnikov, K. Sengupta, A. Silva, and M. Vengalattore, Colloquium: Nonequilibrium dynamics of closed interacting quantum systems, Rev. Mod. Phys. **83**, 863 (2011).
[42] A. Keesling *et al.*, Quantum Kibble-Zurek mechanism and critical dynamics on a programmable Rydberg simulator, Nature (London) **568**, 207 (2019).
[43] J. A. P. Glidden, C. Eigen, L. H. Dogra, T. A. Hilker, R. P. Smith, and Z. Hadzibabic, Bidirectional dynamic scaling in an isolated Bose gas far from equilibrium, Nat. Phys. **17**, 457 (2021).
[44] B. Ko, J. W. Park, and Y. Shin, Kibble-Zurek universality in a strongly interacting Fermi superfluid, Nat. Phys. **15**, 1227 (2019).
[45] C.-R. Yi, S. Liu, R.-H. Jiao, J.-Y. Zhang, Y.-S. Zhang, and S. Chen, Exploring Inhomogeneous Kibble-Zurek Mechanism in a Spin-Orbit Coupled Bose-Einstein Condensate, Phys. Rev. Lett. **125**, 260603 (2020).
[46] M. Motta, C. Sun, A. T. K. Tan, M. J. ORourke, E. Ye, A. J. Minnich, F. G. S. L. Brandão, and G. K.-L. Chan, Determining eigenstates and thermal states on a quantum computer using quantum imaginary time evolution, Nat. Phys. **16**, 205 (2020).
[47] H. Nishi, T. Kosugi, and Y.-i. Matsushita, Implementation of quantum imaginary-time evolution method on NISQ devices by introducing nonlocal approximation, npj Quantum Inf. **7**, 85 (2021).
[48] M. Huo and Y. Li, Shallow Trotter circuits fulfil error-resilient quantum simulation of imaginary time, arXiv:2109.07807; with IBM quantum experience website, https://quantum-computing.ibm.com/ (2021).
[49] X. Y. Pei Zeng and Jinzhao Sun, Universal quantum algorithmic cooling on a quantum computer, arXiv:2109.15304.
[50] E. A. Martinez, C. A. Muschik, P. Schindler, D. Nigg, A. Erhard, M. Heyl, P. Hauke, M. Dalmonte, T. Monz, P. Zoller, and R. Blatt, Real-time dynamics of lattice gauge theories with a few-qubit quantum computer, Nature (London) **534**, 516 (2016).
[51] P. Weinberg, M. Tylutki, J. M. Rönkkö, J. Westerholm, J. A. Åström, P. Manninen, P. Törmä, and A. W. Sandvik, Scaling and Diabatic Effects in Quantum Annealing with a D-Wave Device, Phys. Rev. Lett. **124**, 090502 (2020).
[52] M. Dupont and J. E. Moore, Quantum criticality using a superconducting quantum processor, arXiv:2109.10909.
[53] A. A. Zhukov, S. V. Remizov, W. V. Pogosov, and Y. E. Lozovik, Algorithmic simulation of far-from-equilibrium dynamics using quantum computer, Quantum Inf. Process. **17**, 223 (2018).
[54] H. Lamm and S. Lawrence, Simulation of Nonequilibrium Dynamics on a Quantum Computer, Phys. Rev. Lett. **121**, 170501 (2018).
[55] A. Chiesa, F. Tacchino, M. Grossi, P. Santini, I. Tavernelli, D. Gerace, and S. Carretta, Quantum hardware simulating four-dimensional inelastic neutron scattering, Nat. Phys. **15**, 455 (2019).
[56] C. De Grandi, A. Polkovnikov, and A. W. Sandvik, Universal nonequilibrium quantum dynamics in imaginary time, Phys. Rev. B **84**, 224303 (2011).
[57] C. D. Grandi, A. Polkovnikov, and A. W. Sandvik, Microscopic theory of non-adiabatic response in real and imaginary time, J. Phys. Condens. Matter **25**, 404216 (2013).
[58] C.-W. Liu, A. Polkovnikov, and A. W. Sandvik, Quasi-adiabatic quantum Monte Carlo algorithm for quantum evolution in imaginary time, Phys. Rev. B **87**, 174302 (2013).

[59] S. Yin, P. Mai, and F. Zhong, Universal short-time quantum critical dynamics in imaginary time, Phys. Rev. B **89**, 144115 (2014).

[60] H. K. Janssen, B. Schaub, and B. Schmittmann, New universal short-time scaling behaviour of critical relaxation processes, Z. Phys. B **73**, 539 (1989).

[61] Z. B. Li, L. Schülke, and B. Zheng, Dynamic Monte Carlo Measurement of Critical Exponents, Phys. Rev. Lett. **74**, 3396 (1995).

[62] E. V. Albano, M. A. Bab, G. Baglietto, R. A. Borzi, T. S. Grigera, E. S. Loscar, D. E. Rodriguez, M. L. R. Puzzo, and G. P. Saracco, Study of phase transitions from short-time nonequilibrium behaviour, Rep. Prog. Phys. **74**, 026501 (2011).

[63] S. Zhang, S. Yin, and F. Zhong, Generalized dynamic scaling for quantum critical relaxation in imaginary time, Phys. Rev. E **90**, 042104 (2014).

[64] Y.-R. Shu, S. Yin, and D.-X. Yao, Universal short-time quantum critical dynamics of finite-size systems, Phys. Rev. B **96**, 094304 (2017).

[65] Y.-R. Shu and S. Yin, Short-imaginary-time quantum critical dynamics in the J-Q_3 spin chain, Phys. Rev. B **102**, 104425 (2020).

[66] P. Weinberg and A. W. Sandvik, Dynamic scaling of the restoration of rotational symmetry in Heisenberg quantum antiferromagnets, Phys. Rev. B **96**, 054442 (2017).

[67] A. W. Sandvik, Computational studies of quantum spin systems, AIP Conf. Proc. **1297**, 135 (2010).

[68] E. Farhi, D. Gosset, I. Hen, A. W. Sandvik, P. Shor, A. P. Young, and F. Zamponi, Performance of the quantum adiabatic algorithm on random instances of two optimization problems on regular hypergraphs, Phys. Rev. A **86**, 052334 (2012).

[69] Y. Tang and A. W. Sandvik, Confinement and Deconfinement of Spinons in Two Dimensions, Phys. Rev. Lett. **110**, 217213 (2013).

[70] B. Zheng, Generalized Dynamic Scaling for Critical Relaxations, Phys. Rev. Lett. **77**, 679 (1996).

[71] T. Tomé and M. J. de Oliveira, Short-time dynamics of critical nonequilibrium spin models, Phys. Rev. E **58**, 4242 (1998).

[72] M. Hasenbusch, Finite size scaling study of lattice models in the three-dimensional Ising universality class, Phys. Rev. B **82**, 174433 (2010).

[73] See Supplemental Material at http://link.aps.org/supplemental/10.1103/PhysRevLett.128.020601 for introductions of the numerical method used, benchmark of the conventional imaginary-time relaxation scaling in the quantum Ising model and additional numerical results to support the key findings highlighted in the main text.

[74] H. Shao, W. Guo, and A. W. Sandvik, Emergent topological excitations in a two-dimensional quantum spin system, Phys. Rev. B **91**, 094426 (2015).

[75] For convenience, the scaling form $D^2(\tau, L) = \tau^{-2\beta/\nu z_u} f(\tau L^{-z_u})$ is reshaped as $D^2(\tau, L) = L^{-2\beta/\nu} f(\tau L^{-z_u})$ by a simple replacement of the scaling variable. Similar replacements are also implemented for other quantities.

[76] M. Oshikawa, Ordered phase and scaling in Z_n models and the three-state antiferromagnetic Potts model in three dimensions, Phys. Rev. B **61**, 3430 (2000).

[77] P. Patil, H. Shao, and A. W. Sandvik, Unconventional U(1) to Z_q crossover in quantum and classical q-state clock models, Phys. Rev. B **103**, 054418 (2021).

[78] F. Léonard and B. Delamotte, Critical Exponents Can Be Different on the Two Sides of a Transition: A Generic Mechanism, Phys. Rev. Lett. **115**, 200601 (2015).

[79] T. Okubo, K. Oshikawa, H. Watanabe, and N. Kawashima, Scaling relation for dangerously irrelevant symmetry-breaking fields, Phys. Rev. B **91**, 174417 (2015).

[80] A. W. Harrow and A. Montanaro, Quantum computational supremacy, Nature (London) **549**, 203 (2017).

[81] F. Arute *et al.*, Quantum supremacy using a programmable superconducting processor, Nature (London) **574**, 505 (2019).

[82] H.-S. Zhong *et al.*, Quantum computational advantage using photons, Science **370**, 1460 (2020).

[83] A. Chiocchetta, M. Tavora, A. Gambassi, and A. Mitra, Short-time universal scaling in an isolated quantum system after a quench, Phys. Rev. B **91**, 220302(R) (2015).

[84] P. Gagel, P. P. Orth, and J. Schmalian, Universal Postquench Prethermalization at a Quantum Critical Point, Phys. Rev. Lett. **113**, 220401 (2014).

[85] B. Sciolla and G. Biroli, Quantum quenches, dynamical transitions, and off-equilibrium quantum criticality, Phys. Rev. B **88**, 201110(R) (2013).

[86] S.-K. Jian, S. Yin, and B. Swingle, Universal Prethermal Dynamics in Gross-Neveu-Yukawa Criticality, Phys. Rev. Lett. **123**, 170606 (2019).

[87] S. Yin and S.-K. Jian, Fermion-induced dynamical critical point, Phys. Rev. B **103**, 125116 (2021).

[88] W. Witczak-Krempa, E. S. Sørensen, and S. Sachdev, The dynamics of quantum criticality revealed by quantum Monte Carlo and holography, Nat. Phys. **10**, 361 (2014).